Effect of ratio gold nanoparticles on the properties and efficiency photovoltaic of thin films of amorphous tungsten trioxide

M. H. Mustafa*, A. A. Shihab
Department of Physics, College of Education for Pure Science / Ibn Al-Haitham, University of Baghdad, Baghdad, Iraq

At a substrate temperature of 320 ° C, a chemical spray pyrolysis approach was applied. to create tungsten oxide thin films on glass substrates with varying Au nanoparticle doping concentrations (0, 0.04 and 0.08 M) that have a thickness of roughly 250 nm. Investigated were the structural and optical characteristics. The films were amorphous to the pure films at the substrate temperature (320 °C), according to X-ray diffraction and remain so even after adding GNPs, because the WO_3 structure is amorphous in all samples, whereas the cubic structure of the gold nanoparticles. The morphology of the films was examined using atomic force microscopy (AFM), which showed a decrease in the grain size of the films doped with gold compared to the thin films before the doping process. a UV-Vis spectrophotometer was used to examine the membranes' optical characteristics between the wavelengths of (300-1000) nm. was the optical energy gap of the films (3.23) eV for tungsten oxide film and decreased after adding nanoscale gold to (3.04, 2.95) eV for films doped with different proportions of Au NPs (0.04, 0.08 M), respectively. Hall testing confirms that with 8 (mM) Gold (Au) doping, WO_3 material of the n type was obtained with a maximum carrier mobility of 219.92(cm^2/Vs) and conductivity of 6.52 $(\Omega.cm)^{-1}$. The I-V characteristics of the photovoltaic formed under illumination were determined by measuring the incident power density (100 mW/cm^2) at varied Au doping levels.

(Received July 19, 2023; Accepted November 1, 2023)

Keywords: Structural, Optical properties, Plasmon, Tungsten trioxide films and gold nanoparticles

1. Introduction

Since metal nanoparticles possess characteristics not present in the same material in bulk form, they have been investigated for decades. the proportion of atoms on the crystal's surface to those buried deep inside is significantly influenced by nanosize. As a result, surface impacts are seen much more clearly. Catalysis is one prominent instance in which a high surface area to volume ratio is a crucial factor [1-3]. The shiny look of metals' smooth surfaces in their bulk state is explained by the entire reflection of light caused by the material's high electron density. Finely separated metals, on the other hand, seem black.as a result of the big surface's recurrent reflection phenomenon, which absorbs light [4]. Metals can absorb light strongly once they are nanometer-sized. movement occurs when the coherent electron's frequency and the electromagnetic field's frequency resonate [5]. In the cases of Au and Ag, which display free-conduction electrons with plasma frequency in the visible area, nanoparticles display color [6]. In contrast, some transition metals in the UV area only exhibit diffuse, poorly defined absorption bands [5]. Metal nanoparticles' color and optical characteristics are caused by surface plasma resonance (SPR), a collective longitudinal excitation of conduction electrons on the nanoparticles' surface [7]. The primary goal of this study is to fabricated (n-WO_3/p-Si) heterojunction with doped tungsten oxide films in various concentrations of gold nanoparticles (0, 0.04, 0.08 M) by using the spray pyrolysis technique, which is one of the processes used to produce and prepare thin films of tungsten trioxide [8-15], as well as to examine the structural, optical, and surface characteristics of the prepared samples.

* Corresponding author: mohammed.h.m@ihcoedu.uobaghdad.edu.iq
https://doi.org/10.15251/JOR.2023.196.623

2. Experimental section

Various molar concentrations of $HAuCl_4$ (chlororic acid) are dissolved in tungsten chloride solution (0.06 M), which is made by dissolving H_2WO_4 powder with distilled water after adding a few drops of ammonia [16] solution and mixing for 30 minutes with a magnetic stirrer until the solution is clear, to prepare Au-WO_3 films. This solution is then ready to deposit WO_3 and WO_3: Au films on glass substrates with dimensions 2 and 1.5 cm and on substrates p-type single crystal (111) silicon wafers to fabricate WO_3:Au/Si with different ratio of gold (0,4 and 8)mM by Using the spray pyrolysis technique, pure and doped films were deposited by pyrolyzing at 320 °C with a spray rate of 0.15 ml/sec.

WO_3:Au NPs thin films' structural characteristics were investigated using an X-ray diffractometer. Atomic force spectroscopy (AFM) was used to investigate the surface morphological characteristics of the film. Using a UV-Vis spectrophotometer with wavelengths between 300 and 1000 nm, the optical characteristics of thin films were investigated.

3. Results and discussion

3.1. Structural analysis

3.1.1. X-ray diffraction analysis

Figure (1) refers the XRD patterns of WO3 thin films produced at 320 °C with GNPs doping. The findings are consistent with an amorphous structure, according to Ibrahim [17]. WO3 was not improved by the inclusion of Au gold nanoparticles. The absence of XRD peaks indicates that WO3's structure has improved up to an Au concentration of 0.04 m; nevertheless, at this concentration (0.08 mM), WO3's structure has not yet improved., and that the peaks that appeared at Au concentration (0.08 mM) belong to gold nanoparticles, which appeared at 2Θ equal to (38.214) ^{o} and (44.339) $^{o.}$ The produced particles range in size from 9 to 11 nm on average, and the lattice constant value lies between 2.3544 (A^{o}) and 2.0385 (A^{o}).

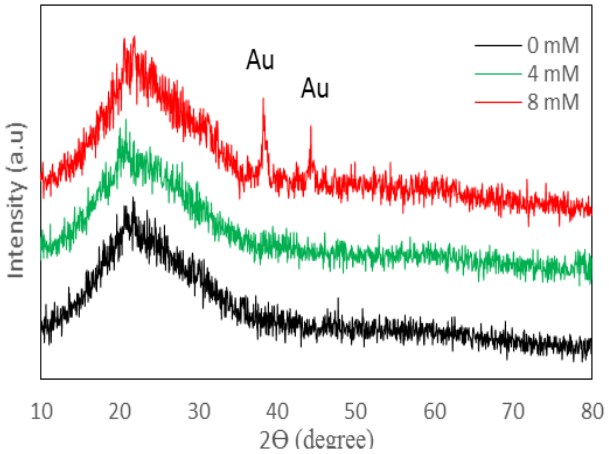

Fig. 1. XRD pattern of the GNPs doped WO_3 thin films with various Au concentrations.

3.1.2. Atomic force microscope (AFM)

The topography of the WO3 surface is depicted in Fig. 2's grain density graph and 3-D WO3:Au atomic force microscope images, which accord with the XRD results. Table 1 shows the average diameter, roughness, and R.M.S. of the samples. The pure WO_3 specimen is tightly packed on the surface, has a granular structure, and is fully organized. As indicated in Table 1, it was discovered that doping reduced the grain size, roughness, and RMS, which is consistent with [17,18].

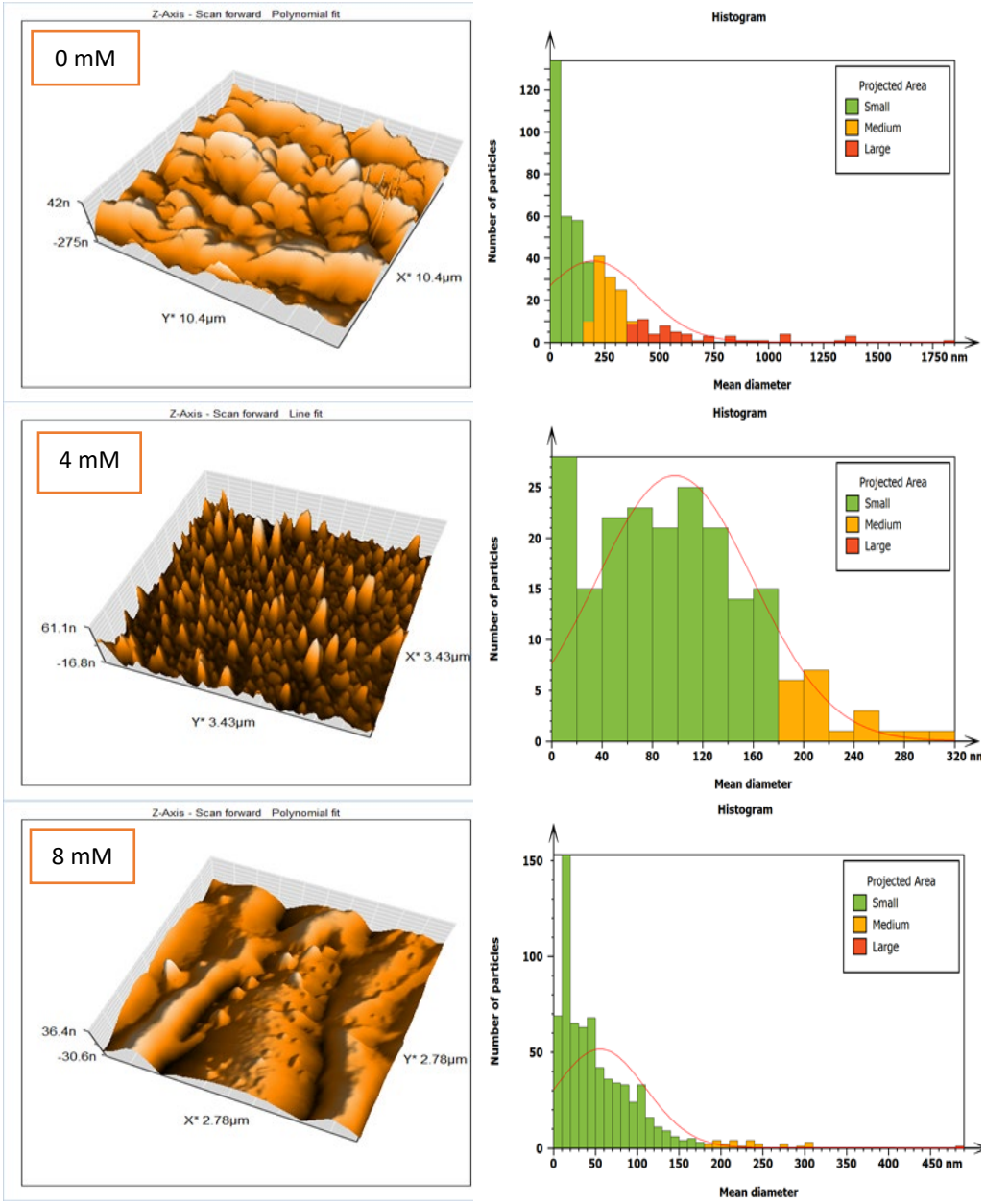

Fig. 2. AFM image and size distribution for WO_3 thin films doped at varied Au thin ratios.

Table 1. AFM characteristics for pure WO_3 and doping at various Au thin ratios.

Au Concentration (mM)	Average diameter (nm)	Roughness Average (nm)	Root mean square (nm)
0	196.2	111.4	143.0
4	97.66	14.76	21.07
8	55.62	42.66	52.56

3.2. Optical studies

The optical characteristics of pure WO_3 thin films and films that have been doped with varying amounts of Au (0, 4, and 8 mM). Measurements were made of this transmission, absorbance, surface plasmon resonance, and optical energy gaps. The films had less transmittance when the Au was applied, as shown by the transmission and absorbance spectrum illustrations in Fig. 3. In general, When Au ratios rise, the transmittance falls. May be a result of greater absorption, which may be related to the deformation brought on by the Au ions in the WO_3.

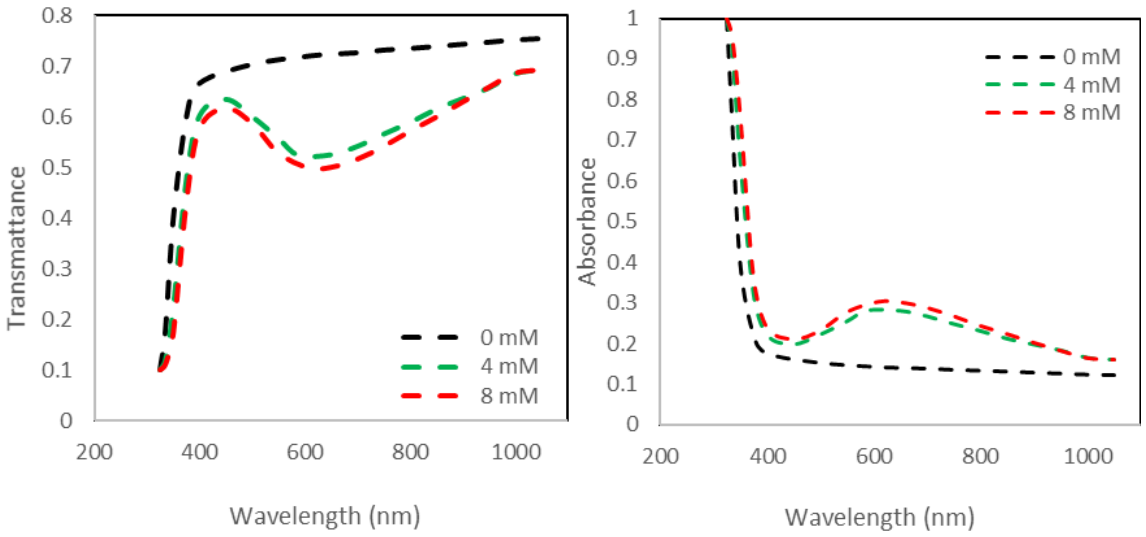

Fig. 3. Transmittance and absorbance spectra of the GNPs doped WO_3 thin films with various Au concentrations.

At substrate temperatures of 320 ^{0}C, Figure 3 displays the optical transmittance and absorbance spectra of tungsten oxide and pure tungsten thin films doped with GNPs. While film doped with 4 mM of gold nanoparticles exhibits low transmittance in the 500–700 nm wavelength range, pure tungsten trioxide film exhibits no transmittance band in this range. With an increase in gold concentration, this transmittance band's intensity gradually increases, reaching its maximum for film doped with 8 mM GNPs. peak location, which is brought on when surface electrons oscillate resonantly irradiated with light of the proper wavelength, has been reported to cause noble metals like silver and gold to exhibit a noticeable response to electromagnetic fields [19]. The basic reason for the light absorption by metal nanoparticles is the coherent oscillation of the conduction band electrons brought on by the interacting electromagnetic field. The absorption band is created when the input photon frequency is in resonance with the collective oscillation of the electrons in the conduction band, which causes the surface plasmon resonance [20, 21]. As a result, the peak position of AuNPs in the tungsten trioxide matrix may be the cause of the increased absorption in the wavelength range of visible region in the gold doped tungsten oxide films. The films' band gap energy (E_g) is determined. The Tauc connection shown below

$$\alpha h\upsilon = A\,(h\upsilon - Eg)^n$$

where α is the absorption coefficient, constant A is the band edge sharpness, h is the Planck's constant; and υ is the radiation frequency. The kind of the optical transition affects the exponent "n". It can be either one of the following values: 1/2, 3/2, 2, or 3.for transitions that are direct permitted, direct forbidden, indirect permitted, and indirect forbidden [22] The optimal straight line part for the Tauc relation in this instance is attained for n = 2 for all films. This demonstrates how these movies use indirect transitions. Since $E_g = h\upsilon$, the optical band gap energy E_g can be calculated by extrapolating the linear region of the plot of $(\alpha h\upsilon))^{1/2}$ vs. photon energy *(hυ)* on the

x-axis. At Ts = 320 ºC, Fig. 4 display the Tauc plots for films made of pure and gold-infused tungsten oxide, and Table 2 displays the computed band gap energies for various films. The band gap energy of the pure tungsten oxide sheet is discovered to be 3.23 eV, and it lowers as gold is added. According to certain findings, the band gap energy of the materials can be impacted by the grain size, crystallinity, and low levels of oxygen in the films [23].

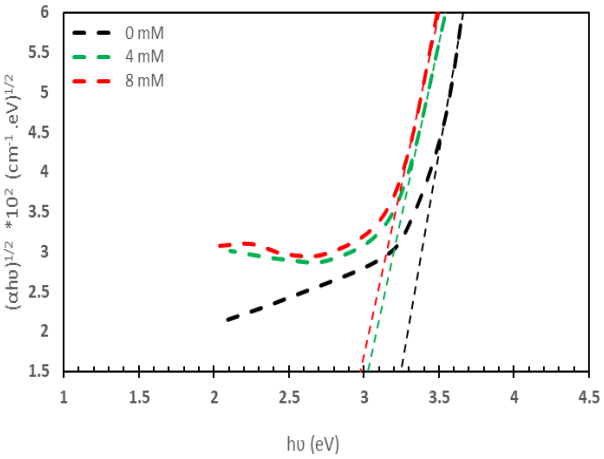

Fig. 4. Energy gap for gold-doped tungsten oxide films and pure films.

The value of energy gap (Eg), full width at half maximum (FWHM) and the LSPR peak location (λ_{SPR}) for all samples were display in table 2.

Table 2. LSPR peak location (λSPR) , full width at half maximum (FWHM) and energy gap for pure WO_3 and doping at various Au thin ratios.

Au Concentration (mM)	E_g (eV)	FWHM (nm)	λ_{SPR} (nm)
0	3.23	Does not appear	Does not appear
4	3.02	328	588
8	2.97	312	608

3.3. Electrical properties

Figure 5 depict the variations in carrier concentration (n_A) and Hall mobility (μ_H) of thin films of un-doped WO_3 and WO_3 doped with various concentrations of Au. Hall measurements reveal that all of these films exhibit a negative Hall coefficient (n-type charge carriers); this result is consistent with [24].

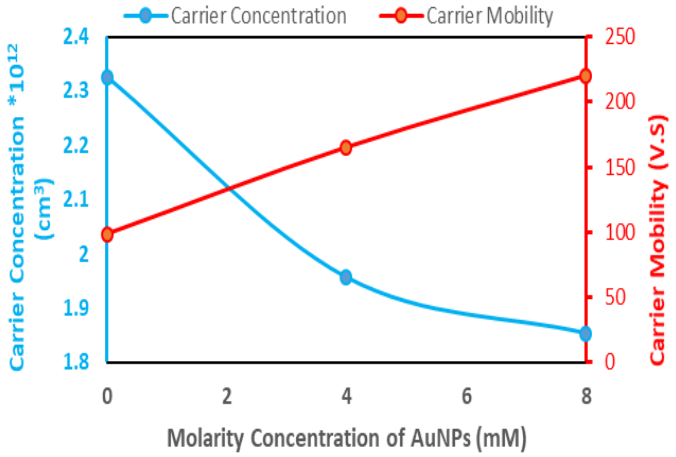

Fig. 5. Pure WO_3 and Au-doped thin film carrier concentration and mobility as a function of Au Molarity concentrations.

Table 3 makes it evident that the doping process has no effect on the kind of charge carriers and that carrier concentration drops with dopant ratio while carrier mobility (μH) increases. The substitution of tungsten for gold may have improved the electrical properties of all samples of WO_3 thin films, as evidenced by higher carrier mobility and conductivity values.

Table 3. Electrical characteristics of pure WO_3 and Au-doped thin films with various Au ratio.

Au Concentration (mM)	$R_H * 10^6$ (cm^3/C)	$n_A \times 10^{12}$ (cm^{-3})	μ_H ($cm^2/V.S$)	$\sigma \times 10^{-5}$ $(\Omega.cm)^{-1}$
0	-2.69	2.33	98.34	3.66
4	-3.20	1.96	164.86	5.16
8	-3.37	1.85	219.92	6.52

Figure 6 displays the current and voltage density of the n-WO_3:Au/p-Si photovoltaic during illumination, with a voltage range of 0 to 0.6 V. Utilizing a photovoltaic with a V_{oc} of 0.55 V and a J_{sc} of 4.44 mA/cm^2. When the Au ratio is 8 mM, the fourth table displays the efficiency is determined to acquire conversion efficiency for solar cells. Because of the sample's increased surface area, as the doping ratios rise, more Au molecules may be absorbed. It can be useful to encourage faster electron transit while minimizing the possibility of electron-hole pair recombination since sunlight aids in improving the efficiency of solar cell production.

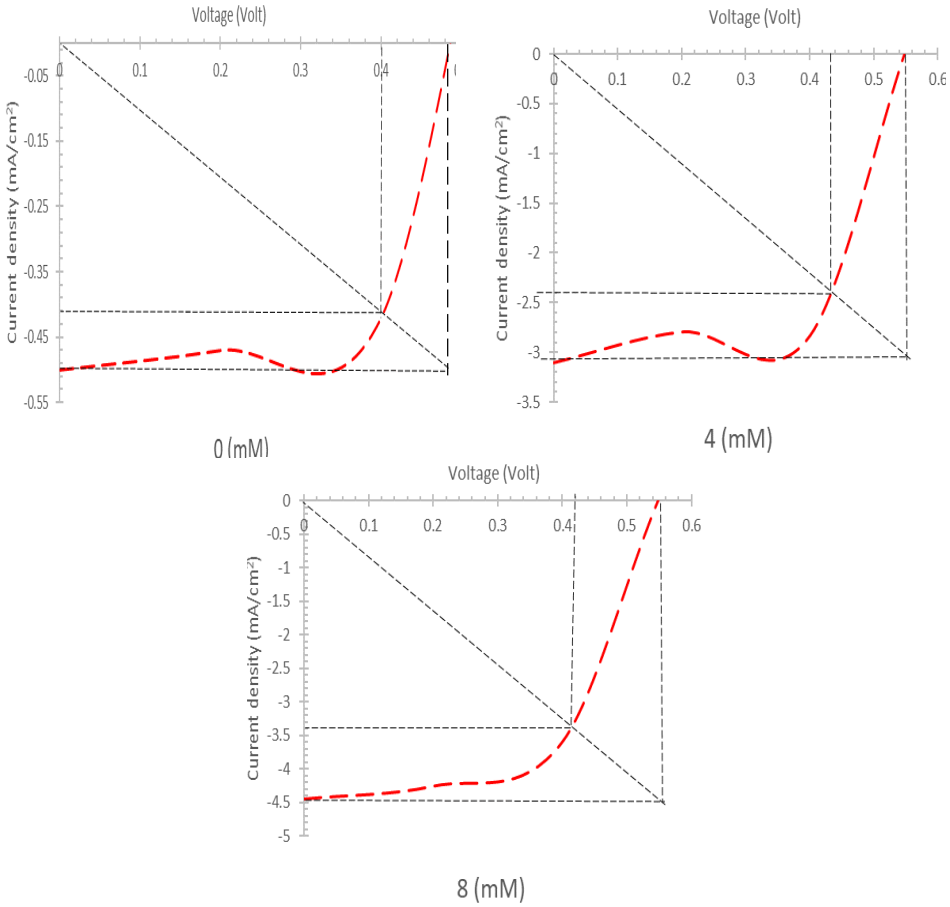

Fig. 5. J-V characteristics for pure WO_3 and Au-doped thin film heterojunction.

Table 4. Factors of the WO_3:Au/Si heterojunction for pure and Au-doped WO_3 thin films in solar cells.

Au Concentration (mM)	J_{SC} (mA/cm^2)	V_{OC} (volt)	J_m (mA/cm^2)	V_m (Volt)	Ƞ %
0	0.5	0.485	0.405	0.4	0.162
4	3.1	0.55	2.4	0.43	1.032
8	4.44	0.55	3.4	0.42	1.428

4. Conclusion

On glass and silicon wafers substrates, pure tungsten trioxide films with a concentration of 0.06 M from WO3 doped with various ratios of gold nanoparticles were successfully made at 320 °C. All of the pure and doped samples' X-ray diffraction patterns for the pure and doped films created at Ts = 320 °C exhibit an amorphous structure. In tungsten trioxide films that were doped with gold nanoparticles in various ratios, the phenomena of surface plasmonic resonance was seen, and it was discovered that the addition of gold decreased the energy gap and particle size. Current-Voltage properties for heterojunction (n-WO_3:Au/p-Si) at 100 (mW/cm^2) incoming power density with maximum efficiency (1.428 %) are achieved due to the heterojunction's superior crystallite size, improved absorption coefficient, low resistivity, and high mobility values.

References

[1] Dugleux, P. de Alameda Marques, S., Powder Technology,.27 (1), 45-52, (1980); https://doi.org/10.1016/0032-5910(80)85040-6

[2] Iman Hameed Khudayer, Bushra Hashem Hussein Ali, Mohammed Hamid Mustafa, Ayser Jumah Ibrahim, Ibn Al-Haitham J. for Pure & Appl. Sci., Vol.31 (1) 2018; https://doi.org/10.30526/31.1.1848

[3] Mohammed Hamid Mustafa, Ibn Al-Haitham J. for Pure & Appl. Sci., Vol. 27 (3) 2014.

[4] J. Jakobi, A. Menéndez-Manjón, V.S.K. chakravadhanula, L. Kienle, P. Wagener, S. Barcikowski, Nanotech 22, 145601-145607, (2011); https://doi.org/10.1088/0957-4484/22/14/145601

[5] J. Jakobi,S. Petersen, A. Menéndez-Manjón, P. Wagener, S. Barcikowski, Langmuir 26(10), 6892-6897 (2010); https://doi.org/10.1021/la101014g

[6] W.G. Zhang, Z.G. Jin, Sci. China Ser. B (47),159-165 (2004); https://doi.org/10.1360/03yb0135

[7] D. Poondi, T. Dobbins, J. Singh, J. Mater. Sci., 35(24), 6237-6243, (2000); https://doi.org/10.1023/A:1026701915796

[8] Hiba M. Ali,I. H. Khudayer, Ibn Al-Haitham Journal for Pure and Applied Sciences. IHJPAS. 36(2)2023; https://doi.org/10.30526/36.2.2990

[9] AA Shehab, SA Maki, AA Salih, Ibn Al-Haitham Journal for Pure and Applied Science 27(2)2017.

[10] Liqaa S Ali, Aliyah A Shehab, Ahmed N Abd, Journal of Physics: Conf. Series 1234 (2019); https://doi.org/10.1088/1742-6596/1234/1/012050

[11] Amun Amri, et al, Ceramics International,45,(2019),12888-12894; https://doi.org/10.1016/j.ceramint.2019.03.213

[12] Liqaa S. Ali, Aliyah A. Shehab, Ahmed N. Abd, Journal of Global Pharma Technology|2019| Vol. 11,224-230.

[13] H. M. Ali and M. H. Mustafa, Chalcogenide Lett., 20(6), pp. 431–437, (2023). https://doi.org/10.15251/CL.2023.206.431

[14] H. K. Hassuna, M. H. Mustafaa, R. H. Athabb, B. K. H. Al-Maiyalya, and B. H. Husseina, J. Ovonic Res., 18(4,) pp. 601–608, (2022). https://doi.org/10.15251/JOR.2022.184.601

[15] A. Z. Obaid, M. H. Mustafa, and H. K. Hassun, "Studying the effect of the annealing on Ag2Se thin film," in AIP Conference Proceedings, AIP Publishing, 2020. Accessed: Oct. 17, 2023. [Online]. Available: https://pubs.aip.org/aip/acp/article-abstract/2307/1/020007/698376

[16] Md. Arifuzzaman, Investigation of Silver Doping on Structural, Optical and Electrical Properties of Spray Deposited Tungsten Trioxide Thin Films, 2021.

[17] I. M. Ibrahim, Iraqi J. Phys., vol. 16, no.36, pp. 11-28, 2018; https://doi.org/10.30723/ijp.v16i36.22

[18] Saadallah F. Hasan, Abdul-Majeed E Al-Samarai A. S. Obaid, Asmiet Ramizy, IOP Conference Series: Materials Science and Engineering ,2021.

[19] R. Jolly Bose, V.S. Kavitha, C. Sudarsanakumar, V.P. Mahadevan Pillai, Applied Surface Science 379 (2016) 505-515; https://doi.org/10.1016/j.apsusc.2016.04.100

[20] S. Basu, S.K. Ghosh, S. Kundu, S. Panigrahi, S. Praharaj, S. Pande, S. Jana, T. Pal, J. Colloid Interface Sci. 313 (2007) 724; https://doi.org/10.1016/j.jcis.2007.04.069

[21] U. Kreibig, M. Vollmer, Optical Properties of Metal Clusters, Springer, Berlin, 1995; https://doi.org/10.1007/978-3-662-09109-8

[22] J. I. Pankove, Optical Processes in semiconductor, Dover publications, New York,1971.

[23] A. Subrahmanyam, A. Karuppasamy, Solar Energy Materials and Solar Cells, 91 (2007), 266-274; https://doi.org/10.1016/j.solmat.2006.09.005

[24] Ganbavle et al., Journal of materials engineering and performance, 23, 1204-1213, (2014); https://doi.org/10.1007/s11665-014-0873-3